Proceedings of the 10th International Conference on Heat Transfer, Fluid Mechanics and Thermodynamics
HEFAT2014
14 – 26 July 2014, Orlando, Florida

HEFAT2014-1569868053

PERFORMANCE MODEL OF SHAMS I SOLAR POWER PLANT

Sara Al-Hanaei
Mechanical Engineering Department
Khalifa University
PO Box 20274, Al Ain, UAE

Sara Al-Shomali
Mechanical Engineering Department
Khalifa University
PO Box 854, Abu Dhabi, UAE

Mohammad Abutayeh
Mechanical Engineering Department
Khalifa University
PO Box 127788, Abu Dhabi, UAE

ABSTRACT

A study of Shams I solar power plant in Abu Dhabi has been conducted to generate a performance model via a spreadsheet. The plant consists of 192 loops containing single-axis parabolic trough collectors. These collectors track the sun and focus sunlight onto a Heat Transfer Fluid (HTF) flowing in an absorber running in their focal line. That causes the temperature of the HTF to rise, which then heats the water flowing in a separate loop. This results in the formulation of vapor that is sent to a turbine. A generator is connected to the shaft of the turbine and it generates electricity due to the rotation of the shaft (caused by the expanding steam) [1]. The spreadsheet computes the annual output of the plant in 1-hour increments. Input data columns include: solar radiation, ambient temperature, humidity, wind speed, time of day, day of year, and other geographical and optical constants.

Keywords: parabolic trough collectors, concentrated solar power, solar energy.

INTRODUCTION

Solar power is the conversion of sunlight energy to electricity. Sunlight can be converted directly to electricity using photovoltaics (PV) or indirectly using concentrated solar power (CSP). The PV technology mainly works by converting sunlight to electric current using the photoelectric effect. Photovoltaics were initially, and still are, used to power small and medium-sized applications. They are an important and relatively inexpensive source of electrical energy where grid power is inconvenient, unreasonably expensive to connect, or simply unavailable. On the other hand, CSP normally focuses sun's energy to boil water, which is then used to provide power [2]. In CSP, electrical power is produced when the concentrated light is converted to heat, which drives a heat engine, usually a steam turbine, connected to an electrical power generator [3]. From the effectiveness point of view, the cost of PV systems is decreasing more rapidly nowadays [4]. Nonetheless, the CSP option was selected for Shams I, due to the low efficiency and the oscillating output of PV systems [5].

THE ABU DHABI ECONOMIC VISION 2030

Under the guidance of His Highness Sheikh Khalifa bin Zayed Al Nahyan, president of the UAE and ruler of Abu Dhabi, and His Highness Sheikh Mohamed bin Zayed Al Nahyan, crown prince of Abu Dhabi, deputy supreme commander of the UAE armed forces and chairman of the Abu Dhabi Executive Council, the Government of Abu Dhabi published a long-term plan for a tremendous transformation of the Emirate's economy. This plan is entitled: *The Abu Dhabi Economic Vision 2030* [6].

The 2030 economic vision emphasizes a reduced reliance on the oil sector as a source of economic activity [6]. It also initiates a greater focus on knowledge-based industries in the future, such as its aim to have 7 % of the total energy capacity of Abu Dhabi supplied through renewable energy by 2020. Examples of renewable energies are: wind, solar, and nuclear energy.

Shams I solar power plant spells the beginning of the 2030 plan's success story, which has a significant future impact on the UAE's economy. "The inauguration of Shams 1 is a major milestone in our country's economic diversification and a step towards long-term energy security" Sheikh Khalifa said [7].

Apparently, the year 2030 represents an important milestone for Abu Dhabi. Baseline growth assumptions reveal that Abu Dhabi could achieve tangible levels of economic diversification by that time [8].

ABOUT SHAMS I

Shams I concentrated solar power plant is currently the largest single-unit CSP plant in the world and the first of its kind in the Middle East [9]. It is located in the western region of Abu Dhabi in the United Arab Emirates, and occupies an area of 2.5 km². It is a joint venture between Masdar™ (60%), Total™ (20%), and Abengoa Solar™ (20%), and is designed and developed by Shams Power Company [10]. What makes Shams I different is the fact that it is the only grid connected solar power plant built in the Middle East. Its location was chosen to be deep in the desert and not near the sea, because of the degrading effect of humidity on incident solar radiation. As a result, a dry-cooling system is used in the power cycle rather than a cooling tower [1].

Shams I uses the parabolic trough collector (PTC) technology to concentrate solar thermal radiation from direct incident sunlight making the plant among the largest PTC plants in the world [11]. The solar field (SF) consists of 192 parallel loops, where each loop contains four solar collector assemblies (SCA) connected in series. An general schematic of Shams I is shown in Figure 1. In addition to the typical components of a PTC-based CSP plant, Shams I includes two unique features related to the use of natural gas (NG). The SF includes 7 NG-Fired heaters on stand-by in case power generation is needed beyond sunshine hours. Also, the power block (PB) includes 2 NG-Fired boosters designed to further raise the temperature of superheated steam heading for the turbine; therefore, boosting the thermal efficiency of the power cycle by sensible heating. Unlike the heaters, the boosters are always on during operation.

Shams I has a net capacity of 100 MWe, which is able to power 20,000 homes in the UAE [7]. By using solar power, up to 175,000 tons of CO_2 emissions are avoided every year, which is equivalent to planting 1.5 million trees or taking 15,000 cars off the road [1].

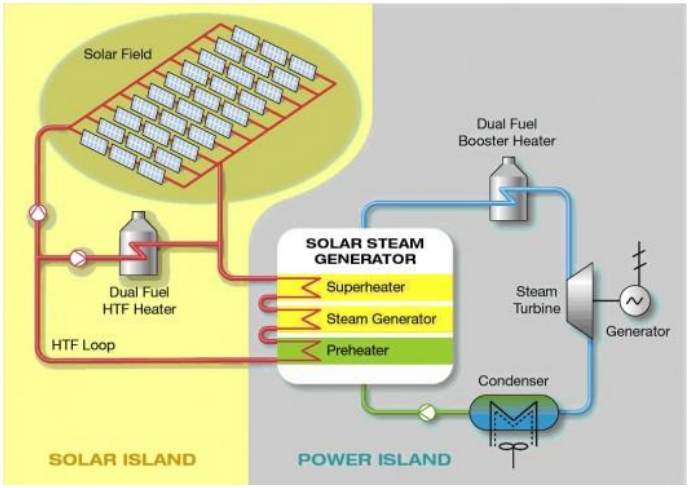

Figure 1: A schematic of Shams I CSP plant

OBJECTIVE

The purpose of this study is to accurately build a performance model of Shams I power plant detailing its annual operation. A spreadsheet has been formulated to show the hourly output of Shams I over an entire typical metrological year (TMY). A performance model shows whether actual generation meets the design criteria. Ideally, the output of the performance model should resemble actual generation. If it doesn't, that would point to either modeling inaccuracy or operational problem. Therefore, a well-developed performance model can help in investigating design flaws, operational issues, as well as finding exactly where the problem is. A well-built performance model can also predict future generation if fed with properly predicted weather data. Furthermore, it is a main feature of the development process as it evaluates tradeoffs earlier in the construction phase based on actual measurements [12].

CALCULATION

The succeeding computations will be performed on each time increment, which in this case is one hour. The purpose of the first set of equations is to compute the direct incident insulation (DII). DII represents all the sunlight that falls on the absorber, or captured solar radiation. In order to do that, several values must be determined. Time correction (TC) is a term that is used to adjust regular time to solar time, since most countries do not lie exactly on the longitudinal line of the earth. It is a function of the longitude angle, time zone (TZ), and day of year and can be calculated as follows:

$$TC = 4(15TZ - l) + 9.87\sin(2X) - 7.53\cos(X) - 1.5\sin(X)$$
$$\text{where: } \mathrm{X} = \frac{2\pi}{365}(Day - 81) \qquad (1)$$

The solar day (SD) is another needed term found by:

$$SD = \begin{cases} Day, \ 0 \le Hour + \frac{TC}{60} \le 24 \\ Day - 1, \ Hour + \frac{TC}{60} < 0 \ AND \ Day > 1 \\ Day + 364, \ Hour + \frac{TC}{60} < 0 \ AND \ Day \le 1 \\ Day + 1, \ Hour + \frac{TC}{60} > 24 \ AND \ Day < 365 \\ 1, \ Hour + \frac{TC}{60} > 24 \ AND \ Day \ge 365 \end{cases} \quad (2)$$

The solar hour (SH) will be used later and is given by:

$$SH = \begin{cases} Hour + \frac{TC}{60}, \ 0 \le Hour + \frac{TC}{60} \le 24 \\ 24 + Hour + \frac{TC}{60}, \ Hour + \frac{TC}{60} < 0 \\ Hour + \frac{TC}{60} - 24, \ Hour + \frac{TC}{60} > 24 \end{cases} \quad (3)$$

The following solar angles are needed to be included in the model. Declination (δ) is the angle between the earth's sun line and the plane through the equator. Hour angle (HA) is a conversion term from hour to angle. Altitude angle (α) is the angle between a line collinear with the sun's rays and the horizontal plane. Azimuth angle (z) is the angle between a due south line and the projection of the site to the sun line on the horizontal plane. Altitude transverse (AT) angle is defined below. These solar angles are calculated as follows:

$$\delta = \sin^{-1}\left[0.398 \cdot \cos\left(0.986 \cdot \frac{\pi}{180} \cdot [SD - 173]\right)\right] \quad (4)$$

$$HA = \frac{\pi}{180} \cdot 15 \cdot (SH - 12) \quad (5)$$

$$\alpha = \sin^{-1}[\sin(\delta) \cdot \sin(\lambda)] + \cos(\delta) \cdot \cos(HA) \cdot \cos(\lambda) \quad (6)$$

$$z = \begin{cases} \pi - \sin^{-1}\left[\frac{-\cos(\delta) \cdot \sin(HA)}{\cos(\alpha)}\right], \ \cos(HA) \ge \frac{\tan(\delta)}{\tan(\lambda)} \\ 2\pi + \sin^{-1}\left[\frac{-\cos(\delta) \cdot \sin(HA)}{\cos(\alpha)}\right], \ \cos(HA) < \frac{\tan(\delta)}{\tan(\lambda)} \end{cases} \quad (7)$$

$$AT = \begin{cases} \alpha, \ |z - \pi| < 1 \\ \tan^{-1}\left(\frac{\tan(\alpha)}{\left|\cos\left(\frac{\pi}{2} + z\right)\right|}\right), \ |z - \pi| \ge 1 \end{cases} \quad (8)$$

The shadow effects on incident solar radiation are evaluated via the shadow argument (SA). SA is a function of PTC row distance (RD), that is the distance between the centers of the PTC, and the aperture width (AW), that is the projected width of the PTC, as well as the AT solar angle defined above. It is found by:

$$SA = \frac{RD}{AW} \cdot \cos\left(\frac{\pi}{2} - AT\right) \quad (9)$$

To account for PTC shadowing that upsets the SF during sunrise and sunset, we need to adjust the incident solar radiation by measuring the shadow efficiency (η_{Shadow}). This is calculated as follows:

$$\eta_{Shadow} = \begin{cases} 1, \ SA \ge 1 \\ 0, \ SA < 0 \\ SA, \ 0 \le SA < 1 \end{cases} \quad (10)$$

The incident angle (IA) is the angle between solar beams and the line normal to PTC aperture. It is constantly changing and can be found by:

$$\mathrm{IA} = \cos^{-1}\left[\sqrt{1 - [\cos(\alpha - \mathrm{Tilt}) - \mathrm{Y} \cdot \cos(\mathrm{Tilt})\cos(\alpha)]^2}\right] \quad (11)$$
$$\text{where: } \mathrm{Y} = 1 - \cos[\mathrm{z} - \mathrm{Orientation}]$$

Another term used to adjust the incident solar radiation is the incident angle modifier (IAM). It accounts for the direct and indirect losses due to the IA and is estimated by the following correlation:

$$IAM = \cos(IA) - 0.000525\left(\frac{180}{\pi} IA\right) - 0.0000286\left(\frac{180}{\pi} IA\right)^2 \quad (12)$$

End loss efficiency ($\eta_{End\ Loss}$) is yet another term used to adjust incident solar radiation. It accounts for radiation that is incident on the PTC, but reflected off the absorber. It has higher values in the summer when the sun is more overhead and has lower values in the winter when the sun is more inclined. It is given by:

$$\eta_{End\ Loss} = 1 - \frac{FL}{L_{SCA}} \cdot tan(IA) \quad (13)$$

Where FL is the focal length of the PTC and L_{SCA} is the overall length of the SCA.

Combining the previous adjustment terms, the absolute efficiency ($\eta_{Absolute}$) is given by:

$$\eta_{Absolute} = \eta_{Optical} \cdot \eta_{Shadow} \cdot \eta_{End\ Loss} \cdot C_{Mirror} \cdot IAM \quad (14)$$

DII is then calculated by

$$DII = \eta_{Absolute} \cdot DNI \quad (15)$$

Now that the value of DII is obtained, the following equation is used in order to calculate the amount of heat available for collection where the availability term takes out the collectors that are out of service:

$$\mathrm{q_{DII}} = \frac{\mathrm{N_{SCA\ per\ SF}} \cdot \mathrm{L_{SCA}} \cdot (\mathrm{AW_{SCA}} - \mathrm{Gap_{SCA}}) \cdot \mathrm{Availability} \cdot \mathrm{DII}}{1{,}000{,}000} \quad (16)$$

Heat loss from SCA absorbers and pipes cannot be disclosed; however, there are many examples in literatures, such as the expressions included within NREL's SAM solar modeling software.

$$\mathrm{q_{SCA\ Loss}} = \mathrm{f}(\varphi) \quad (17)$$

$$\mathrm{q_{Pipe\ Loss}} = \mathrm{f}(\varphi) \quad (18)$$

Where φ is the temperature difference between the HTF and ambient air calculated as:

$$\varphi = T_{HTF} - T_A \quad (19)$$

Heat loss in NG heaters and boosters must be taken into consideration and is estimated by:

$$q_{NG\ Loss} = R_{NG\ Heater\ Loss} \cdot q_{NG\ Heater} + R_{NG\ Booster\ Loss} \cdot q_{NG\ Booster} \quad (20)$$

Each R represents a heat loss ratio. These ratios are usually very small, usually around 1%, since NG heat exchangers are very well insulated.

HTF properties will not be disclosed; however, they are also available in literature as functions of temperature.

$$h_{HTF} = f(T_{HTF}) \quad (21)$$

$$\rho_{HTF} = f(T_{HTF}) \quad (22)$$

The heat collected in the SF equals the amount of heat available for collection minus the heat losses, subject to the capacity of the heat exchanger (HX) of course.

$$q_{SF} = min\left\{Z1, max\left\{q_{DII} - q_{SCA\ Loss} - q_{Pipe\ Loss}, 0\right\}\right\} \quad (23)$$
$$where: Z1 = N_{HX} \cdot Overload_{HX} \cdot Capacity_{HX}$$

The NG-Fired heaters of the SF are off during normal operation. Heat produced by those SF heaters will be set to zero in the current model since Shams I has no plans for nighttime generation at the moment.

$$q_{NG\ Heater} = 0 \quad (24)$$

On the other hand, the NG-Fired boosters of the PB are on during normal operation. The heat demand of those PB boosters is clearly proportional to the heat collected in the SF. It can be calculated by conducting an energy balance on the SF heat exchangers and the NG-Fired boosters separately, then solving for the mass flow of water through each heat exchanger train. The mass flow of water through both heat exchanger trains is the same; therefore, they are set equal to each other producing the following expression, subject to booster's capacity.

$$q_{NG\ Booster} = min\left\{Z2, \frac{h_{H2O}^{Booster} - h_{H2O}^{Return}}{h_{H2O}^{Return} - h_{H2O}^{Supply}} \cdot q_{SF \to PB}\right\} \quad (25)$$
$$where: Z2 = N_{Booster} \cdot Overload_{Booster} \cdot Capacity_{Booster}$$

Subscripts *Booster*, *Return*, and *Supply* refer to steam conditions at booster exit, HX exit, and HX inlet. Superheated steam enthalpies are available in literature, such as the ASME 1967 steam tables as functions of temperature and pressure.

$$h_{H2O} = f(T_{H2O}, P_{H2O}) \quad (26)$$

The amount of heat sent to the PB is obtained by combining the different heat sources: NG-Fired heaters, NG-Fired boosters, and heat collected in the SF.

$$q_{PB} = q_{SF} + q_{NG\ Heater} + q_{NG\ Booster} \quad (27)$$

The overall heat produced by NG comprises heat produced in SF heaters and PB boosters as well as heat loss by both schemes.

$$q_{NG} = q_{NG\ Heater} + q_{NG\ Booster} + q_{NG\ Loss} \quad (28)$$

The annual mass of NG burned can be found by dividing the overall heat produced with NG by its mass-based lower heating value.

$$M_{NG} = \frac{3600 \cdot \int_0^\infty q_{NG}}{LHV_{NG}} \quad (29)$$

NG is mainly made up of methane that burns according to the following reaction:

$$CH_4 + 2\ O_2 \rightarrow CO_2 + 2\ H_2O$$

So, the molar amount of CO_2 produced equals the molar amount of NG burned in line with the above combustion reaction. Therefore, the annual mass of CO_2 produced equals the annual mass of NG burned multiplied by the ratio of their molecular weights.

$$M_{CO_2} = \frac{M_{NG} \cdot MW_{CO_2}}{MW_{NG}} \quad (30)$$

The ratio of power produced by NG in relation to total power production totalized annually is usually capped by the government and can be found by:

$$R_{NG-PB} = \frac{\int_0^\infty q_{NG}}{\int_0^\infty q_{PB}} \quad (31)$$

SF efficiency is defined as:

$$\eta_{SF} = \begin{cases} 0, & DNI = 0\ OR\ q_{DII} = 0 \\ \frac{q_{SF}}{q_{DII}} \cdot \frac{DII}{DNI}, & DNI \neq 0\ AND\ q_{DII} \neq 0 \end{cases} \quad (32)$$

Cycle efficiency, or PB thermal efficiency, represents proprietary information belonging to Shams I that cannot be disclosed. Heat balances data from Shams I were obtained and regressed producing a cycle efficiency correlation that is a function of PB thermal load and ambient temperature. Cycle degradation is also included in the expression to account for equipment aging. It is given as a percent and can be assumed to equal zero for newly built power plants.

$$\eta_{Cycle} = (1 - CD) \cdot f(q_{PB}, T_A) \quad (33)$$

Gross electric generation rate is calculated by multiplying cycle efficiency by the PB thermal load, subject to electric generation limits.

$$w_{Gross} = \begin{cases} 0, \ \eta_{Cycle} \cdot q_{PB} < w_{Gross}^{Minimum} \\ \eta_{Cycle} \cdot q_{PB}, \ w_{Gross}^{Minimum} \leq \eta_{Cycle} \cdot q_{PB} \leq w_{Gross}^{Maximum} \\ w_{Gross}^{Maximum}, \ \eta_{Cycle} \cdot q_{PB} > w_{Gross}^{Maximum} \end{cases} \quad (34)$$

A small fraction of the generated electricity is used to run plant auxiliary equipment. That amount of that electricity is known as auxiliary or parasitic load. Detailed power consumption data of different plant equipment is needed to calculate it; however, it can be reasonably estimated as a percent of gross generation.

$$\mathrm{w_{Aux}} = (1 - \eta_{\mathrm{Gross \rightarrow Net}}) \cdot \mathrm{w_{Gross}} \quad (35)$$

Net electric generation rate is calculated by subtracting the auxiliary load from gross generation.

$$\mathrm{w_{Net}} = \mathrm{w_{Gross}} - \mathrm{w_{Aux}} \quad (36)$$

Total net electric generation is obtained by integrating the net electric generation rate over the desired period. In this model, total annual net electric generation is calculated by:

$$W_{Net} = \int_0^{\infty} w_{Net} \quad (37)$$

In the previous equations, the symbol ∞ was used to indicate the upper integration limit. As will be seen in the next section, integration or energy accumulation will be done on daily, monthly, and annual basis.

RESULTS

A spreadsheet was created where the above equations were applied to hourly increments for an entire year. So, 8760 rows are included in the spreadsheet, one row for each hour of the year. In addition to TMY data such as ambient temperature and DNI, variables given in Table 1 were input to the spreadsheet model.

Table 2 lists the annually totalized model results. The annual solar resource is 1.93 MWh/m², 66% of which is exploitable - 1.28 MWh/m². The absorber tubes in the SF are exposed while the piping is very well insulated. Consequently, heat loss from the SF was 109 GWh, while piping heat loss was 19 GWh. In addition, 1 GWh was lost to the ambient from the NG system.

There was no heat input from the SF NG-Fired heaters as was assumed before, but there was 121 GWh heat input from the PB NG-Fired boosters.

The SF supplied 535 GWh to the PB while it dumped 9 GWh of heat by defocussing collectors at times when available solar heat exceeded PB heat capacity. The total amount of heat processed by the PB was 656 GWh producing a 250 GWh of gross electricity, or 225 GWh of net electricity.

The plant was on for 2582 hours, or 29% of the time, while it was off for 6178 hours, or 71% of the time. The plant ran at maximum capacity for 558 hours, 6% of the time, or 22% of the operating time. 10K tons of NG was burned producing 27K tons of CO_2. A conventional combined cycle power plant at the same capacity would have produced 138K tons of CO_2. Overall, approximately 21% of the generated power was attributed to NG.

Table 1: Model inputs

Input Variable	Value	Unit
C_{Mirror} =	90%	
$\eta_{Optical}$ =	75%	
Availability =	99%	
$R_{NG\ Heater\ Loss}$ =	1%	
$R_{NG\ Booster\ Loss}$ =	1%	
CD =	0%	
$\eta_{Gross \rightarrow Net}$ =	90%	
N_{HX} =	4	
$Overload_{HX}$ =	100%	
$Capacity_{HX}$ =	75	MW_{th}
$N_{Booster}$ =	2	
$Overload_{Booster}$ =	100%	
$Capacity_{Booster}$ =	50	MW_{th}
$q_{PB}^{Minimum}$ =	50	MW_{th}
$q_{PB}^{Maximum}$ =	350	MW_{th}
$w_{Gross}^{Minimum}$ =	10	MW_e
$w_{Gross}^{Maximum}$ =	125	MW_e
P_{H2O}^{Supply} =	113	bar
P_{H2O}^{Return} =	108	bar
$P_{H2O}^{Booster}$ =	103	bar
T_{H2O}^{Supply} =	219	°C
T_{H2O}^{Return} =	380	°C
$T_{H2O}^{Booster}$ =	542	°C
T_{HTF}^{Supply} =	293	°C
T_{HTF}^{Return} =	393	°C
$N_{Loops\ per\ SF}$ =	192	
$N_{SCA\ per\ Loop}$ =	4	
Δt =	1	h
TZ =	4	h
l =	54.37	°
λ =	23.57	°
Tilt =	0	°
Orientation =	0	°
L_{SCA} =	150	m
FL_{SCA} =	1.71	m
AW_{SCA} =	5.77	m
Gap_{SCA} =	0.32	m
RD =	17.20	m
MW_{CO2} =	44.011	g/mol
MW_{NG} =	16.858	g/mol

Table 2: Annual outputs

Output Variable	Value	Unit
Σ DNI =	1.93	MWh_{th}/m^2
Σ DII =	1.28	MWh_{th}/m^2
$Q_{SCA\ Loss}$ =	109	GWh_{th}
$Q_{Pipe\ Loss}$ =	19	GWh_{th}
$Q_{NG\ Loss}$ =	1	GWh_{th}
Q_{Heater} =	0	GWh_{th}
$Q_{Booster}$ =	121	GWh_{th}
Q_{SF} =	535	GWh_{th}
$Q_{Defocus}$ =	9	GWh_{th}
Q_{PB} =	656	GWh_{th}
W_{Gross} =	250	GWh_e
W_{Net} =	225	GWh_e
ON =	2,582	hours
OFF =	6,178	hours
Max =	558	hours
M_{NG} =	10,236	ton
M_{CO2} =	26,723	ton
R_{NG-PB} =	21%	

Table 3 lists the monthly heat input and electric output of Shams I. Evidently, the monthly thermal energy input from the SF and the NG boosters in the summer season, May-September, is higher than that in the winter season, November-January. Naturally, there is more incident solar radiation in the summer since the sun is more overhead and has less declination. Hence, there is less end loss, known as cosine loss, in the summer as was presented earlier. On the other hand, the sun has more declination in the winter and a lot of radiation is reflected off the absorber. Also, the local weather in Abu Dhabi entails more cloudy conditions in winter than summer. Table 3 also shows that the summer season represents an optimum period of electric generation for the solar plant. Fortunately, this coincides with increased power demand during summer times in Abu Dhabi due to increased air conditioning use.

Heat loss correlations describing heat loss rates from SCA absorbers and pipes to the ambient were not disclosed in this paper; however, their results can be exposed. Figure 2 shows heat loss from SCA absorbers and pipes versus the temperature gradient between the HTF and ambient air. Heat loss from SCA absorbers is much more prevalent than heat loss from pipes since absorbers are exposed while pipes are insulated.

Cycle efficiency data, also known as heat balances, describing PB thermal efficiency as a function of thermal load and ambient temperature were not disclosed in this paper; however, their results can be exposed. Figure 3 and Figure 4 relate cycle efficiency to both ambient temperature and heat load, respectively. Cycle efficiency dependence on PB heat load is much more streamlined than its dependence on ambient temperature suggesting that cycle efficiency depends more on PB heat load than it does on ambient temperature.

Table 3: Monthly outputs

Month	Q_{SF} MWh_{th}	Q_{NG} MWh_{th}	Q_{PB} MWh_{th}	W_{Gross} MWh_e	W_{Net} MWh_e
January	21,229	5,333	25,294	9,727	8,754
February	35,924	9,082	43,068	16,854	15,168
March	33,704	8,481	40,321	15,647	14,082
April	43,245	10,900	52,106	19,729	17,757
May	66,832	16,946	80,881	30,485	27,437
June	67,609	17,210	82,217	30,917	27,825
July	59,693	15,164	72,241	27,327	24,594
August	61,340	15,621	74,622	28,631	25,768
September	55,785	14,257	67,960	26,677	24,009
October	46,516	11,793	55,976	21,992	19,793
November	31,394	7,913	37,493	14,562	13,105
December	20,692	5,025	23,726	9,184	8,265

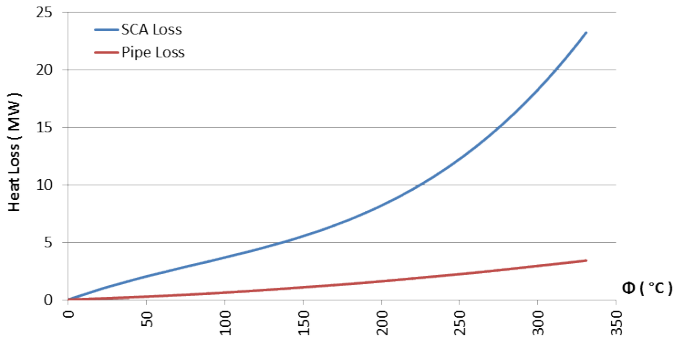

Figure 2: Heat loss from SCA absorbers and SF pipes

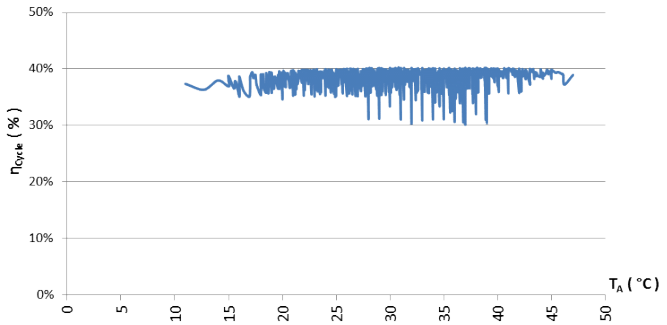

Figure 3: η_{Cycle} dependence on ambient temperature

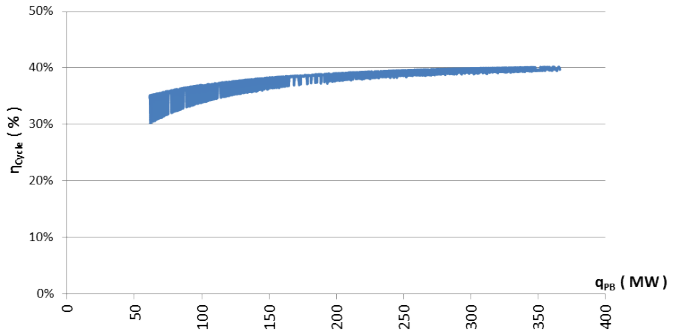

Figure 4: η_{Cycle} dependence on PB heat load

Figure 5 illustrates the daily thermal energy input from the SF with a dome-shaped graph. It appears that there are significantly high thermal energy levels from the sun approximately between end of April and half way through November. The preceding period represents an optimum period of total thermal energy input apparently as it is free of oscillations. On the other hand, there are many oscillations in the period between the beginning of a year and half way through April as well as in the period between middle November and the end of a year. The higher the oscillations, the less thermal energy collected from the SF. This might be merely due to the presence of clouds in the winter and spring seasons. It should be noted that dust and humidity degrade the overall thermal energy input as well, but don't cause oscillations. Dust and humidity are both rampant in Abu Dhabi.

Figure 6 shows the amount of NG Shams I is burning in the PB boosters. PB boosters are there to increase the turbine inlet steam temperature from 380 ºC to 540 ºC, therefore enhancing the thermal efficiency of the power cycle [13]. Apparently, Figure 6 is analogous to Figure 5 because the amount of NG used in the PB boosters corresponds to the amount of heat collected in the SF as was seen earlier. It is worth mentioning that Shams I use of NG is limited to 600,000 MMBTU or 176 GWh. The current model predicts NG consumption to be around 122 GWh between boosters and heat loss. A previous study [14] has also concluded that NG will supply 18% of the PB thermal load. The current model predicts that NG will supply 21% of the PB thermal load as mentioned earlier and as shown in Table 2.

Figure 7 indicates the daily amount of electrical energy produced from Shams I CSP plant. Figure 7 resembles both Figure 5 and Figure 6 to some extent since electric generation represents a percentage of PB heat load. One more interesting observation can be inferred from Figure 7. Its dome, located in the middle of the summer, has a flat top due to SF defocussing. If available solar heat exceeds the thermal capacity of the PB, some of the SF collectors are taken out of focus to limit the influx of solar heat. It is desired to keep defocussing to absolute minimum because it amounts to thermal energy dumping; however, it is a necessary evil sometimes.

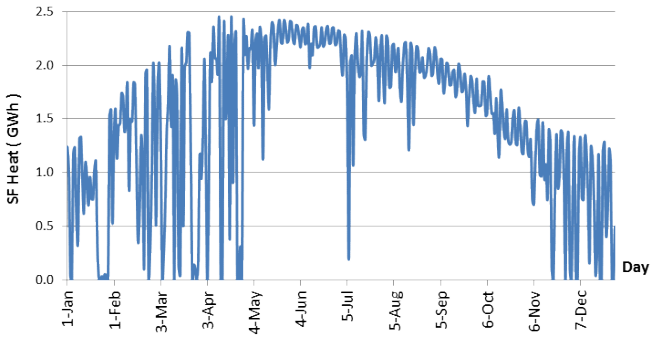

Figure 5: Daily heat collected by the SF

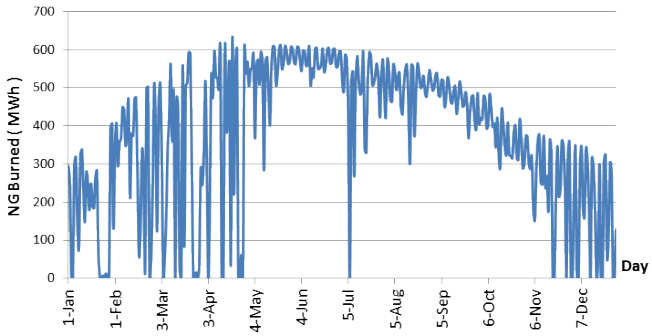

Figure 6: Daily heat delivered by PB NG-Fired boosters

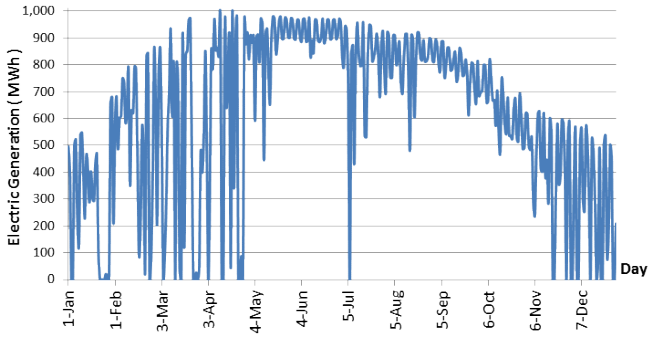

Figure 7: Daily net electric generation of Shams I

CONCLUSION

To sum up, a performance model of Shams I solar power plant has been built. The technique used to create the model involves applying the above equations in 1-hour increments based on TMY weather data input. Graphs representing the thermal energy input and the electrical energy output were obtained for a typical year.

The developed model represents a useful tool that would be beneficial in many cases. It can be used for predicting power plant generation when provided with forecast weather data. It can also be used to evaluate plant performance by comparing its modeled output to actual generation; thereby, helping identify sources of errors and troubleshoot performance issues.

The developed performance model has been applied in 1-hour increments for an entire year; however, it can be applied in different increments and over different periods. For example, the performance model can be applied in 5-minute increments for a whole day to gage daily performance. Increment size should be carefully selected since calculations are carried out incrementally. Very large increments will introduce more uncertainty while very small increments will introduce more output oscillations, which is not exactly true. Output oscillations are rare in reality due to plant thermal inertia.

NOMENCLATURE

A	ambient
AT	altitude transverse, radians
Availability	operating collectors, percent
AW	SCA aperture width, m
C	SCA mirror cleanliness, percent
Capacity	thermal capacity, MW
CD	cycle degradation, percent
CSP	concentrating solar power
Day	day of year, day
DII	direct incident insolation, W/m²
DNI	direct normal insolation, W/m²
FL	SCA focal length, m
Gap	SCA middle gap, m
h	enthalpy, kJ/kg
HA	hour angle, radians
Hour	hour of day, hour
HTF	heat transfer fluid
HX	heat exchanger
IA	incident angle, radians
IAM	incident angle modifier, percent
l	longitude, degrees
L	length, m
LHV	lower heating value, kJ/kg
M	mass, kg
MW	molecular weight, g/mol
N	count
NG	natural gas
Orientation	SCA orientation angle, radians
Overload	overload capability, percent
P	pressure, bar
PB	power block
PTC	parabolic trough collector
PV	photovoltaics
q	heat flow, MW
Q	thermal energy, MWh
R	heat loss or heat flow ratio, percent
RD	SCA row distance, m
SA	shadow argument
SCA	solar collector assembly
SD	solar day, day
SF	solar field
SH	solar hour, hour
T	temperature, °C
TC	time correction term, minute
Tilt	SCA tilt angle, radians
TMY	typical metrological year
TZ	time zone, hour
w	electric work flow, MW
W	electrical energy, MWh
z	azimuth angle, radians
α	altitude angle, radians
∆t	time increment, hour
δ	declination angle, radians
η	efficiency, percent
λ	latitude angle, radians
ρ	density, kg/m³
φ	temperature difference, °C

REFERENCES

[1] Quick, D., 2013, “World’s largest concentrated solar power plant opens in the UAE.”, from http://www.gizmag.com/shams-1-worlds-largest-concentrated-solar-power-plant/26707

[2] Energy.gov, n.d., “SOLAR”, from http://energy.gov/science-innovation/energy-sources/renewable-energy/solar

[3] Sandia National Laboratories, n.d., “Solar Recycling of Carbon Dioxide into Hydrocarbon Fuels.”, from http://energy.sandia.gov/wp/wp-content/gallery/uploads/S2P_SAND2009-5796P.pdf

[4] Energysmith, n.d., “Investors favour PV over CSP.”, from http://www.energysmith.net/articles/investorspv-csp.pdf

[5] Abutayeh, M., Goswami, Y. D. and Stefanakos, E. K., 2013, “Solar thermal power plant simulation.”, Environ. Prog. Sustainable Energy, 32, pp. 417-424.

[6] The Abu Dhabi Council for economic development, 2009, “The Abu Dhabi Economic Vision 2030.”, from https://www.abudhabi.ae/egovPoolPortal_WAR/appmanager/ADeGP/Citizen?_nfpb=true&_pageLabel=p_citizen_homepage_hidenav&did=131654&lang=en

[7] AlMakahleh. S., 2013, “UAE President inaugurates Shams 1, region's largest concentrated solar power project.”, from http://gulfnews.com/uae-president-inaugurates-shams-1-region-s-largest-concentrated-solar-power-project-1.1159328

[8] The Government of Abu Dhabi, 2009, “The Abu Dhabi Economic Vision 2030.”, from http://gsec.abudhabi.ae/Sites/GSEC/Content/EN/PDF/Publications/economic-vision-2030-executive-summary-mandate2,property=pdf.pdf

[9] Shamspower, 2010, “Press releases issues since June 2010.”, from http://www.shamspower.ae/en/media-centre/

[10] Masdar.ae, n.d., “Shams I” from http://www.masdar.ae/en/city/detail/shams-1

[11] Spiegel ONLINE, 2013, “Abu Dhabi: Riesiges Sonnenwärmekraftwerk geht in Betrieb.”, from http://www.spiegel.de/wissenschaft/technik/abu-dhabi-riesiges-sonnenwaermekraftwerk-shams-1-nimmt-betrieb-auf-a-889386.html

[12] Microsoft Developer Network, 2013, “Chapter 2 - Performance Modeling.”, from http://msdn.microsoft.com/en-us/library/ff647767.aspx

[13] Goebel. O., Luque. F., n.d., “Shams One 100 MW CSP Plant in Abu Dhabi.”, from http://cms.solarpaces2012.org/proceedings/paper/dab772327aa

[14] Quick. D., 2010, “100MW concentrated solar power plant to be built in the UAE.”, from http://www.gizmag.com/shams-1-concentrated-solar-power-plant/1538